LETTERS

Early geochemical environment of Mars as determined from thermodynamics of phyllosilicates

Vincent Chevrier[1], Francois Poulet[2] & Jean-Pierre Bibring[2]

Images of geomorphological features that seem to have been produced by the action of liquid water have been considered evidence for wet surface conditions on early Mars[1]. Moreover, the recent identification of large deposits of phyllosilicates, associated with the ancient Noachian terrains[2,3] suggests long-timescale weathering[4] of the primary basaltic crust by liquid water[2,5]. It has been proposed that a greenhouse effect resulting from a carbon-dioxide-rich atmosphere sustained the temperate climate required to maintain liquid water on the martian surface during the Noachian[6,7]. The apparent absence of carbonates and the low escape rates of carbon dioxide[8], however, are indicative of an early martian atmosphere with low levels of carbon dioxide. Here we investigate the geochemical conditions prevailing on the surface of Mars during the Noachian period using calculations of the aqueous equilibria of phyllosilicates. Our results show that Fe^{3+}-rich phyllosilicates probably precipitated under weakly acidic to alkaline pH, an environment different from that of the following period, which was dominated by strongly acid weathering[9] that led to the sulphate deposits identified on Mars[10–12]. Thermodynamic calculations demonstrate that the oxidation state of the martian surface was already high, supporting early escape of hydrogen. Finally, equilibrium with carbonates implies that phyllosilicate precipitation occurs preferentially at a very low partial pressure of carbon dioxide. We suggest that the possible absence of Noachian carbonates more probably resulted from low levels of atmospheric carbon dioxide, rather than primary acidic conditions[13]. Other greenhouse gases may therefore have played a part in sustaining a warm and wet climate on the early Mars.

Phyllosilicates, especially clay minerals, are usual products of the weathering process, resulting from the interaction between the atmosphere, the hydrosphere and the lithosphere. Impact-driven hydrothermalism may also form clays in the subsurface[14]. Although this process is unlikely to explain the OMEGA (Observatoire pour la Minéralogie, l'Eau, les Glaces et l'Activité) observations of deposits of several hundred square kilometres not correlated to impacts[2], it still involves liquid water, mostly from meteoric or surface origin. Here we discuss a potential aqueous weathering process that might have leached the primary minerals to form the phyllosilicates detected on the surface of Mars. During leaching, fractionation of elements occurs because water removes ions progressively from primary silicates, according to their solubility. Soluble ions like K^+, Na^+, Ca^{2+} or Mg^{2+} are dissolved first, leaving less soluble ions like Fe^{3+}, Al^{3+} and H_4SiO_4 (silica) to precipitate as phyllosilicates[15]. Therefore, phyllosilicates can be used as indicators of the degree of ion leaching by liquid water on the surface of Mars. The detection by OMEGA of Mg/Fe smectites primarily, as well as montmorillonite, $Ca_{0.167}(Al_{1.67}Mg_{0.33})Si_4O_{10}(OH)_2$ (ref. 2), containing both insoluble (Fe^{3+}, Al^{3+}) and soluble (Mg^{2+} and Ca^{2+}) ions, indicates weak fractionation of elements and thus moderate leaching. In neutral to alkaline conditions (see below), the calculated solubility of smectites is less than 10^{-7} g l^{-1}. The combination of low solubility with moderate leaching suggests that the weathering process occurred at a moderate water-to-rock ratio. Very high water-to-rock ratios would have led to Al-rich phyllosilicates such as kaolinite (only tentatively detected once by OMEGA). Indeed, kaolinite is deprived of soluble ions and contains only Al^{3+} and silica, indicating a drastic leaching of all soluble ions, and its very low solubility (10^{-14} g l^{-1} at pH = 7) allows it to precipitate in extremely dissolved systems.

The main chemical parameters most likely to control the precipitation of phyllosilicates are mineral, water and atmospheric compositions, as well as the temperature of the solution. The formation of iron smectite nontronite mostly depends on the oxidation–reduction and pH conditions (Fig. 1). In addition to these fundamental parameters, aluminium, iron and silica activities have a strong influence on the precipitation of nontronite. Berthierine is the usual Fe^{2+}-phyllosilicate in reducing pedogenetic environments[4,16,17]. The equilibrium between berthierine and nontronite is mainly dependent on the aluminium concentration. The presence of nontronite is only possible when the activity of aluminium becomes sufficiently low, at most 10^{-5} (Fig. 1a). Thus, at high Fe (0.8×10^{-3}) and low Al^{3+} (10^{-25}) activities, nontronite precipitates at pH values between 4 and 10, that is, in slightly acidic to alkaline conditions. Nontronite also involves precipitation of the Fe^{3+} phase rather than the Fe^{2+} phase, indicating much lower iron solubility (activity of 10^{-10}). In such higher oxidation conditions, nontronite is forced to precipitate at higher pH values of at least 6 (Fig. 1b). However, nontronite could also precipitate in subsurface environments[2], in equilibrium with endogenic Fe^{2+}-phyllosilicates such as greenalite or minnesotaite (Fig. 1c). In this case, the most significant difference is the appearance of ferrihydrite in the system, and the possibility that nontronite could precipitate at even higher pH values, up to 12 (Fig. 1c). Such environments usually present higher temperatures, which shift the stability field of nontronite towards a lower pH (about one unit at 100 °C, Fig. 1c).

Silica activity has a strong influence on smectite precipitation. High silica activities allow nontronite to precipitate only at low pH, down to 3 at the saturation relative to amorphous silica (Fig. 2). Such low-pH conditions are often associated with the formation of sulphates observed at the surface of Mars[9,11,12]. Indeed, the presence of SO_2 generates strongly acidic waters that inhibit the formation of nontronite, and favours Fe^{3+} sulphates. Partial pressures of SO_2 as low as 10^{-8} bar generate waters with pH values of ~2–3 and high SO_4^{2-} activities. These values are clearly in the stability field of jarosite (Fig. 3)[18]. In conclusion, the presence of nontronite indicates the following conditions: (1) a low aluminium activity, (2) a high oxidation level, (3) weakly acidic to alkaline conditions and (4) very low abundance of SO_2.

[1]W. M. Keck Laboratory for Space Simulation, Arkansas Center for Space and Planetary Sciences, MUSE 202, University of Arkansas, Fayetteville, Arkansas 72701, USA. [2]Institut d'Astrophysique Spatiale, Université Paris-Sud and CNRS (UMR 8617), F-91405, Orsay, France.

The highly oxidizing conditions required for the precipitation of nontronite imply oxidation of the Fe^{2+} in primary silicates into Fe^{3+}. O_2 and H_2O_2 are the best potential oxidant. However, O_2 abundance in the early martian atmosphere probably remained very low, below 10^{-12} bar (ref. 19). On Earth, it took about 2 billion years for the O_2 level to reach today's high values[20], mostly because of biological activity and photosynthesis. Even in the present oxidizing martian atmosphere, the H_2O_2 density is extremely low[21] (6×10^{-15} cm^{-2}). The most abundant potential oxidant on early Mars is water. Oxidation of Fe^{2+} into Fe^{3+}, even if not thermodynamically favoured, may be driven by thermal escape of H_2, resulting from the reduction of water[22,23], according to the following equation:

$$Fe^{2+}{}_{(aq)} + H_2O = Fe^{3+}{}_{(aq)} + \tfrac{1}{2}H_{2(g)} + HO^-{}_{(aq)} \quad (1)$$

A greenhouse effect of CO_2 can be invoked to maintain liquid water long enough to allow silicate alteration, and phyllosilicate formation. Such a primitive environment has often been proposed to explain the multiple geomorphological evidences of fluvial activity[6] and may have resulted from primary degassing[7,24]. Abundant CO_2 should have led to formation of carbonate deposits, which have not yet been detected by OMEGA. It has been proposed that early Noachian acidic conditions prevented precipitation of carbonates[13]. However, according to our calculations, the smectites observed by OMEGA on the Noachian crust indicate zones where weathering of primary silicates has acted in slightly acidic to alkaline conditions, much more favourable to carbonate formation. The large phyllosilicate-rich deposits are spatially disconnected from the Hesperian

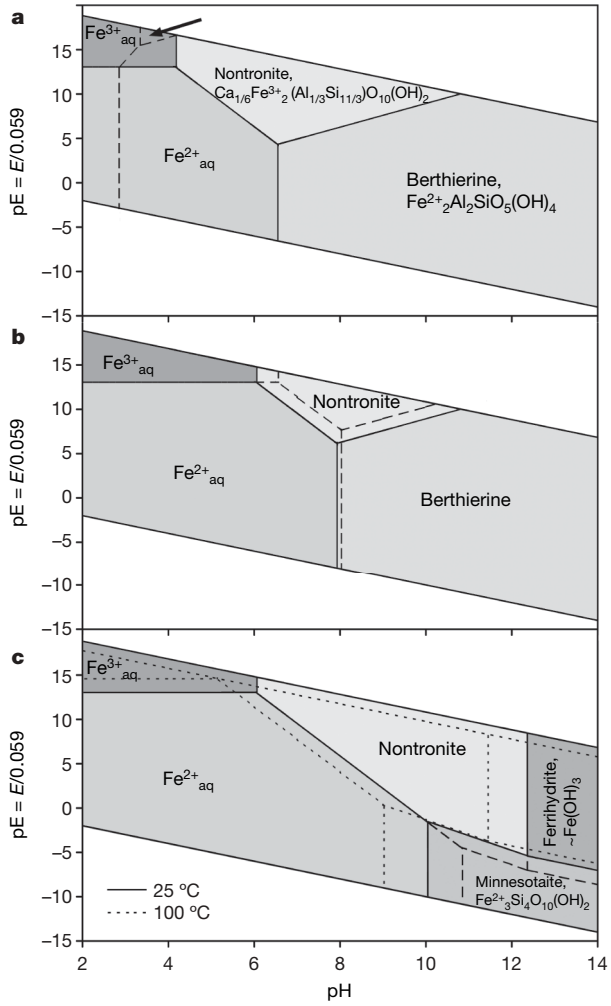

Figure 1 | pE–pH diagrams of nontronite stability at 25 °C with other phases most likely to be present on Mars. These phases are: aqueous Fe^{2+} and Fe^{3+}, berthierine, minnesotaite, greenalite $Fe^{2+}{}_3Si_2O_5(OH)_4$ and ferrihydrite. **a**, Berthierine, with the following aqueous species activities: $\log[Fe] = -3.1$, $\log[H_4SiO_4] = -4.5$, $\log[Al^{3+}] = -25$, $\log[Ca^{2+}] = -3.3$. The black dashed line shows the stability fields for the upper limit of aluminium activity (10^{-5}) needed to still have nontronite. If the activity of Al^{3+} is larger than 10^{-5}, berthierine precipitates in almost all conditions, except for very low pH (below 3) and the stability field of nontronite is extremely restricted (indicated by black arrow). **b**, Low activitiy of iron (10^{-10}) resulting from oxidative conditions, indicated by the presence of Fe^{3+} phases, and for the following silica activities: $\log[H_4SiO_4] = -4.5$ (black lines), $\log[H_4SiO_4] = -5.5$ (dashed lines). **c**, Nontronite forms in equilibrium with endogenic phyllosilicates (minnesotaite and greenalite (dashed lines)) and for $\log[Fe] = -10$, $\log[H_4SiO_4] = -4.5$, $\log[Al^{3+}] = -25$. Endogenic conditions can lead to higher temperatures, so the equilibrium diagram is also calculated with minnesotaite at 100 °C (dotted lines) in the same conditions, using the Van't Hoff relationship[30], assuming that the entropy variation is negligible in the temperature interval[30].

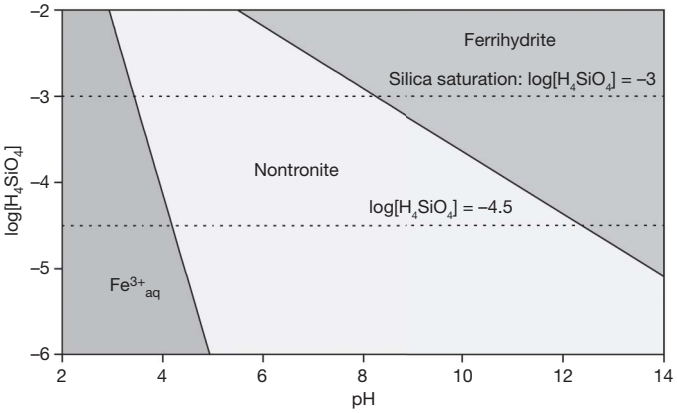

Figure 2 | Stability field of nontronite, aqueous Fe^{3+} and ferrihydrite as a function of dissolved silica activity and pH. Activities of Ca^{2+} and Al^{3+} are the same as for Fig. 1a. The maximum of silica activity is 10^{-3}, where amorphous silica starts to precipitate, whereas 3.2×10^{-5} ($\log[H_4SiO_4] = -4.5$) corresponds to the medium silica activity used to build the pE–pH diagrams showed in Fig. 1.

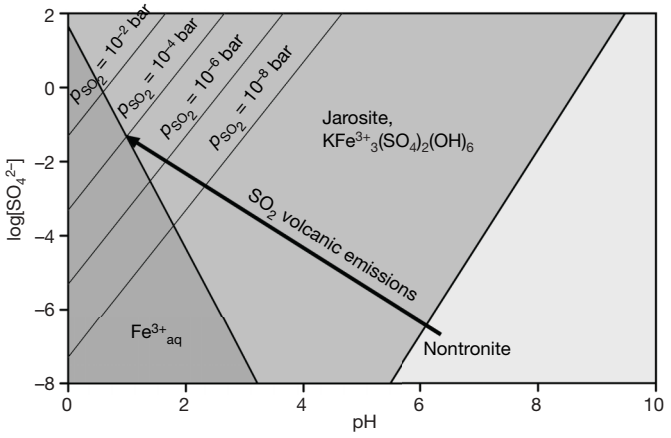

Figure 3 | Equilibrium of nontronite versus jarosite as a function of dissolved sulphate activity (SO_4^{2-}) and pH. Activities of Fe, Al^{3+}, H_4SiO_4 and Ca^{2+} are the same as for Fig. 1a, and $\log[K^+] = -5$. The thin lines represent various partial pressures of SO_2 in equilibrium with water, at a H_2 partial pressure of 10^{-6} bar, according to the following reaction: $SO_2 + H_2O = SO_4^{2-} + 2H^+ + H_2$. The thick arrow represents the evolution of the conditions with increasing pressure of SO_2 if the dissolution of SO_2 is stoichiometric, forcing surface conditions to evolve from neutral-alkaline (nontronite) to acidic and sulphate-rich conditions (jarosite). The large volcanic activity at the end of the Noachian[5,26] has probably inhibited the precipitation of smectites, inducing the formation of the sulphate deposits widely observed in the Hesperian terrains.

sulphate-rich areas[3], where the corresponding pH conditions were too low at ~3–4 (refs 9 and 25) to allow smectite precipitation (Fig. 1).

The late Noachian to early Hesperian (around 3.7 Gyr ago) intense volcanism resulting from the Tharsis rise[26] and other volcanoes has probably injected large amounts of SO_2 into the atmosphere, ending the neutral-weathering period of smectite formation, possibly dissolving the carbonates if present, and shifting the conditions into the sulphate-acidic environment responsible for the sulphates observed in later Hesperian terrains (Fig. 3). Smectites would still be present after this acidic phase during the Hesperian because they are far more resistant to redissolution than carbonates, and mechanical erosion continuously exposes fresh outcrops. Our modelling can also explain *in situ* observations of the Fe^{3+}-bearing phase made by the Mars Exploration Rovers Spirit and Opportunity[27,28] as well as the detection of small phyllosilicate-rich outcrops by OMEGA in Terra Meridiani[2]. These observations indicate localized (in space and time) environments in which dissolved silica activity might have been sufficiently high to produce both phyllosilicates and sulphates. This could result from evaporation processes, efficient in increasing the concentrations of dissolved species[9].

The (pH–p_{CO_2}) aqueous equilibrium between carbonates and smectites provides a direct insight into the CO_2 partial pressure during their formation. The abundance of Mg/Fe-rich smectites[2] probably reflects the primary mineralogy of the martian crust dominated by Mg and Fe silicates. Because the precipitation of nontronite depends on the oxidation–reduction conditions and the pH, the equilibrium between carbonates and Mg,Fe-smectites is a function of the Fe abundance (expressed by the Mg number $x_{Mg} = Mg/(Mg+Fe)$, in mol), and p_{CO_2} (Fig. 4). If only Mg-smectite saponite, $Ca_{0.165}Mg_3(Al_{0.33}Si_{3.67})O_{10}(OH)_2$, precipitates, the equilibrium is independent of the pH value, at a p_{CO_2} of 2.5×10^{-3} bar. Increasing Fe (decreasing x_{Mg}) abundances towards the nontronite end member makes the equilibrium more sensitive to the pH. In this case the Fe-rich smectite can precipitate at higher p_{CO_2} if the pH is higher, and at lower p_{CO_2} in a less neutral environment (Fig. 4). It has been previously demonstrated that the precipitation of nontronite is also strongly sensitive to the silica activity (Fig. 2). Setting the silica activity at the saturation relative to amorphous silica (10^{-3}) provides an upper limit for the p_{CO_2}. Lower silica activity logically favours carbonates, which sets the carbonate–smectite boundary at lower p_{CO_2} (Fig. 4).

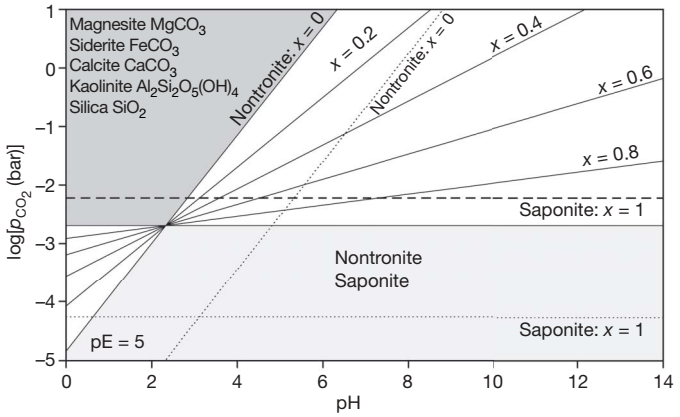

Figure 4 | Equilibrium diagram between carbonates and smectites as a function of the CO_2 partial pressure, the pH and the Mg number, x_{Mg}. ($x_{Mg} = 1$ corresponds to Mg-smectite saponite, whereas $x_{Mg} = 0$ corresponds to Fe-smectite nontronite). Calcite and kaolinite represent accessory phases associated to the Fe,Mg-carbonates (siderite and dolomite), accounting for the excess of Ca^{2+} and Al^{3+} present in the Mg,Fe-smectites. The oxidation potential pE has been set up at 5 (oxidizing water). The silica activity has been set up at the highest value (10^{-3}) corresponding to the saturation relative to amorphous silica, giving an upper limit to the CO_2 partial pressures (thin black lines). If we consider the silica activity of the initial model (3.2×10^{-5}), the equilibrium lines of smectites and carbonates (thin dotted lines) are shifted about two orders of magnitude towards lower CO_2 partial pressures. Both dark grey and light grey zones correspond to exclusive ranges of conditions (for high silica activity) where only carbonates or smectites, respectively, can exist. In the white zone, the equilibrium depends on the composition in Mg and Fe of the smectite/carbonate assemblage. Increasing concentration in Mg (and the Mg number) makes the equilibrium less sensitive to the pH. The horizontal dashed line indicates today's conditions on Mars. Considering the usually quite large error on thermodynamic values (about 0.5 log units), present-day conditions are very close to the equilibrium between Mg-rich smectites and carbonates.

The ALH84001 meteorite is an Mg,Fe-orthopyroxenite ($x_{Mg} \approx 0.8$) of Noachian age. If it is representative of the primary martian crust composition, the p_{CO_2} of the equilibrium between carbonates and smectites is low between 10^{-2} and 10^{-3} atm at silica saturation, and 10^{-5} to 10^{-4} for the lower silica activity (3.2×10^{-5}, Fig. 4). Therefore, the presence of smectites without carbonates, if confirmed when analysed at sample levels (NASA's Mars Science Laboratory and the ESA's Exomars, which are next-generation rovers for the surface exploration of Mars), would suggest that the p_{CO_2} remained low during the Noachian, and thus probably during the entire history of Mars.

A low p_{CO_2} value in the Noachian is not sufficient to sustain a warm and wet atmosphere. Therefore, a sufficient greenhouse effect might require the presence of other gases, such as sulphur dioxide, ammonia and methane. However, ammonia is rapidly photolysed to N_2 and H_2 (ref. 29). The absence of sulphate deposits in the Noachian terrains[5] does not favour a sulphate-rich early Noachian atmosphere (Fig. 3), leaving methane as an alternative[17], provided that a large flux was present.

METHODS

The smectite compositions represent chemical end members most likely to be present on the early Mars[30], according to its primary mafic composition. The thermodynamic values used in the calculations come from various sources (see Supplementary Information). All diagrams were calculated by setting the equilibrium reactions and calculating the corresponding Gibbs free energy of the reaction $\Delta_r G^0_{298\,K,\,1\,bar}$, converted into the reaction constant K (see equations in the Supplementary Information) according to the formula:

$$K = \exp[-\Delta_r G^0_{298\,K,\,1\,bar}/RT] \quad (2)$$

where R is the ideal gas constant and T is the temperature of the reaction. The pH of the equilibrium was calculated from the products of the activities of the dissolved species. For the oxidation–reduction reaction potential E, we used the following formula:

$$E = E^0 + (0.059/n)\log K \quad (3)$$

where n is the number of exchanged electrons. The equilibrium reactions are then plotted in a space in which E is a function of pH such that voltage E divided by 0.059 gives a pH equivalent, that is, an activity of electrons in the solution (pE) rather than a voltage (Fig. 1). Eventually other variables can be used, such as activities of important ions (such as H_4SiO_4 in Fig. 2 or SO_4^{2-} in Fig. 3) or partial pressures (p_{CO_2} in Fig. 4). The temperature effect was determined using the Van't Hoff equation, assuming that the enthalpy variation $\Delta_r H^0_{298\,K,\,1\,bar}$ is negligible in the temperature interval[30]:

$$\ln(K_2/K_1) = (\Delta_r H^0_{298\,K,\,1\,bar}/R) \times (1/T_1 - 1/T_2) \quad (4)$$

Received 29 September 2006; accepted 22 May 2007.

1. Malin, M. C. & Edgett, K. S. Evidence for persistent flow and aqueous sedimentation on early Mars. *Science* **302**, 1931–1934 (2003).
2. Poulet, F. *et al.* Phyllosilicates on Mars and implications for the early Mars history. *Nature* **481**, 623–627 (2005).
3. Bibring, J.-P. *et al.* Mars surface diversity as revealed by the OMEGA/Mars Express observations. *Science* **307**, 1576–1581 (2005).
4. Meunier, A. & El Albani, A. The glauconite–Fe-illite–Fe-smectite problem: a critical review. *Terra Nova* **19**, 95–104 (2006).

5. Bibring, J. P. *et al.* Global mineralogical and aqueous Mars history derived from OMEGA/Mars express data. *Science* **312,** 400–404 (2006).
6. Jakosky, B. M. & Phillips, R. J. Mars' volatile and climate history. *Nature* **412,** 237–244 (2001).
7. Pollack, J. B., Kasting, J. F., Richardson, S. M. & Poliakoff, K. The case for a wet, warm climate on early Mars. *Icarus* **71,** 203–224 (1987).
8. Barabash, S., Fedorov, A., Lundin, R. & Sauvaud, J. A. Martian atmospheric erosion rates. *Science* **315,** 501–503 (2007).
9. Tosca, N. J. *et al.* Geochemical modeling of evaporation processes on Mars: insight from the sedimentary record at Meridiani Planum. *Earth Planet. Sci. Lett.* **240,** 122–148 (2005).
10. Arvidson, R. E. *et al.* Spectral reflectance and morphologic correlations in Eastern Terra Meridiani, Mars. *Science* **307,** 1591–1594 (2005).
11. Gendrin, A. *et al.* Sulfates in Martian layered terrains: the OMEGA/Mars Express view. *Science* **307,** 1587–1591 (2005).
12. Squyres, S. W. *et al.* In situ evidence for an ancient aqueous environment at Meridiani Planum, Mars. *Science* **306,** 1709–1714 (2004).
13. Fairen, A. G. *et al.* Inhibition of carbonate synthesis in acidic oceans on early Mars. *Nature* **431,** 423–426 (2004).
14. Naumov, M. V. Principal features of impact-generated hydrothermal circulation systems: mineralogical and geochemical evidence. *Geofluids* **5,** 165–184 (2005).
15. Eggleton, R. A., Foudoulis, C. & Varkevisser, D. Weathering of basalt: changes in rock chemistry and mineralogy. *Clays Clay Mineral.* **35,** 161–169 (1987).
16. Sheldon, N. D. & Retallack, G. J. Low oxygen levels in earliest Triassic soils. *Geology* **30,** 919–922 (2002).
17. Sheldon, N. D. Precambrian paleosols and atmospheric CO_2 levels. *Precambr. Res.* **147,** 148–155 (2006).
18. Elwood-Madden, M. E., Bodnar, R. J. & Rimstidt, J. D. Jarosite as an indicator for water-limited weathering on Mars. *Nature* **431,** 821–823 (2004).
19. Catling, D. C. & Moore, J. M. The nature of coarse-grained crystalline hematite and its implications for the early environment of Mars. *Icarus* **165,** 277–300 (2003).
20. Kasting, J. F. Earth's early atmosphere. *Science* **259,** 920–926 (1993).
21. Encrenaz, T. *et al.* Hydrogen peroxide on Mars: evidence for spatial and seasonal variations. *Icarus* **170,** 424–429 (2004).
22. Chevrier, V., Rochette, P., Mathé, P.-E. & Grauby, O. Weathering of iron rich phases in simulated Martian atmospheres. *Geology* **32,** 1033–1036 (2004).
23. Lammer, H. *et al.* Loss of water from Mars: implications for the oxidation of the soil. *Icarus* **165,** 9–25 (2003).
24. Phillips, R. J. *et al.* Ancient geodynamic and global-scale hydrology on Mars. *Science* **291,** 2587–2591 (2001).
26. Solomon, S. C. *et al.* New perspectives on ancient Mars. *Science* **307,** 1214–1220 (2005).
27. Wang, A. *et al.* Evidence of phyllosilicates in Wooly Patch, an altered rock encountered at West Spur, Columbia Hills, by the Spirit rover in Gusev crater, Mars. *J. Geophys. Res.* **111,** E02S16, doi:10.1029/2005JE002516 (2006).
28. Glotch, T. D. *et al.* Mineralogy of the light-toned outcrop at Meridiani Planum as seen by the Miniature Thermal Emission Spectrometer and implications for its formation. *J. Geophys. Res.* **111,** E12S03, doi:10.1029/2005JE002672 (2006).
29. Sagan, C. & Chyba, C. The early faint Sun paradox: organic shielding of ultraviolet-labile greenhouse gases. *Science* **276,** 1217–1221 (1997).
30. Gooding, J. L. Chemical weathering on Mars. Thermodynamic stabilities of primary minerals (and their alteration products) from mafic igneous rocks. *Icarus* **33,** 483–513 (1978).

Supplementary Information is linked to the online version of the paper at www.nature.com/nature.

Acknowledgements This work was supported by a grant from the Arkansas Space Center and the Arkansas Space Grant Consortium.

Author Contributions V.C. made the calculations. V.C., F.P. and J.-P.B. wrote the manuscript.

Author Information Reprints and permissions information is available at www.nature.com/reprints. The authors declare no competing financial interests. Correspondence and requests for materials should be addressed to V.C. (vchevrie@uark.edu).